

GPVDM simulation of layer thickness effect on power conversion efficiency of $\text{CH}_3\text{NH}_3\text{PbI}_3$ based planar heterojunction solar cell

A. Hima¹, A. Khechekhouche², I. Kemerchou³, N. Lakhdar¹, B. Benhaoua², F. Rogti³, I. Telli⁴, A. Saadoun⁵

¹ Faculty of Technology, Univ. El-Oued, El oued 39000, ALGERIA

² Renewable Energy Research unite in Arid Zones, El-Oued University, ALGERIA

³ Laboratory of analysis and control of energy systems and networks, Faculty of Technology University of Laghouate, ALGERIA

⁴ Faculty of Technology, University of Biskra, ALGERIA

⁵ Faculty of Technology, University of Sidi Belabbes, ALGERIA

himaek@yahoo.fr

Abstract – Perovskite-based solar cell technologies have been a very attractive area of research in recent years. Organic-inorganic perovskite materials are in an increased evolution in power conversion efficiency. Inorganic materials have been tested at the laboratory level but their power conversion efficiency is still limited. In this paper, we used the GPVDM software to study the effect of some parameters on power conversion efficiency in a planar heterojunction solar cell based on $\text{CH}_3\text{NH}_3\text{PbI}_3$ as an absorbing layer. The modifications were made by considering layers of perovskite without defects. The results show that the efficiency of the power conversion can be improved by adjusting layer thickness; in our case power conversion efficiency was increased from 9.96 % to 12.9 %

Keywords: Perovskite, MAPbI₃, PCE, GPVDM Software, layer thickness

Received: 02/06/2018 – Accepted: 25/06/2018

I. Introduction

The very peculiar structure of perovskites is at the origin of many researches in various fields of physics and their applications. It was discovered in 1940 that synthetic ceramics of perovskite structure such as barium titanate (BaTiO_3) had remarkable piezoelectric properties, that is to say that they were electrically polarized easily under the action of mechanical stresses. Perovskite-type single crystals have been more recently manufactured with even more interesting piezoelectric properties.

The research in laboratories on hybrid organic-inorganic perovskites has become very intensive. This new technology of perovskite solar cells has seen a rapid progression and each time new percentage of power conversion efficiency that appear. To see the surprising progression of this area reminds that in 2009 a study was made on a cell based on $\text{CH}_3\text{NH}_3\text{PbBr}_3$ with a high photovoltage of 0.96 V and the value of the efficiency was 3.8% [1]. After two years in 2011, a Perovskite cell of size 2-3 nm ($\text{CH}_3\text{NH}_3\text{PbI}_3$) nanocrystal gave a solar-electric conversion efficiency of 6.54% [2]. During the year 2013, energy conversion efficiencies reached an astounding 16.2% [3]. In the same year, an optimization of the TiO_2 layer treatment conditions, yields a PCE of 19.3% [4, 6]. Almost five years of research, it became between 22.1 and 22.6 % [7]

Different parameters can increase PCE in perovskite based solar cells; one of them is layer thickness of different layers. In the present paper we used GPVDM which is a powerful software simulation for photovoltaics, where we investigated effect of different layer thickness on power conversion efficiency of a planar heterojunction solar cell using $\text{CH}_3\text{NH}_3\text{PbI}_3$ as absorber layer.

II. Device simulation parameters

General-Purpose Photovoltaic Device Model (GPVDM) is free general purpose software for solar cell simulation based on solving Poisson equation (1) and the bipolar drift diffusion equations (2,3) and the carrier continuity equations (4,5) in 1D and time domain.

$$\frac{d}{dx} \cdot \epsilon_0 \epsilon_r \cdot \frac{d\phi}{dx} = q(n - p) \quad (1)$$

$$J_n = q\mu_c n \frac{\partial E_c}{\partial x} + qD_n \frac{\partial n}{\partial x} \quad (2)$$

$$J_p = q\mu_h p \frac{\partial E_v}{\partial x} - qD_p \frac{\partial p}{\partial x} \quad (3)$$

$$\frac{\partial J_n}{\partial x} = q \left(R_n - G + \frac{\partial n}{\partial t} \right) \quad (4)$$

$$\frac{\partial J_p}{\partial x} = -q \left(R_p - G + \frac{\partial p}{\partial t} \right) \quad (5)$$

More detail on above equation resolving and device modeling can be found in more detail in [8-11].

GPVDM software graphical interface is shown in Figure 1.

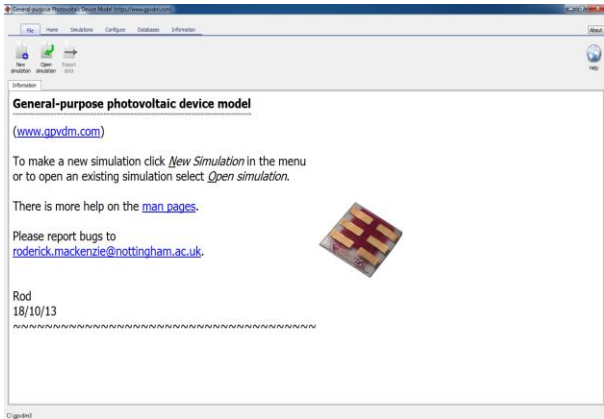


Figure 1. GPVDM Home window.

In Figure 2 is shown the planar heterojunction architecture of a $\text{CH}_3\text{NH}_3\text{PbI}_3$ based solar cell. The layer configuration adopted in this simulation is Glass/TCO/ETM/ $\text{CH}_3\text{NH}_3\text{PbI}_3$ /HTM/Silver where ETM layer is the TiO_2 and the HTM layer is the spiro-OMeTAD. In Table 1 is shown initial parameters that were carefully picked from practical and theoretical references [12-21]. Perovskite electrical and optical parameters are set from [16] and from GPVDM software database based on [22]. Glass layer and silver layer thickness are taken 6×10^{-8} m and 2×10^{-7} m respectively.

Our simulation is based on study of effects of different layer thickness on power conversion efficiency. Initial layer thickness given in Table 1 yields the J-V characteristic curve shown in Figure 3, in which power conversion efficiency PCE is 9.96 %, fill factor is 75.86 %, Open-circuit voltage V_{oc} is 0.47 V and short-circuit density of current is -277 A/m^2 .

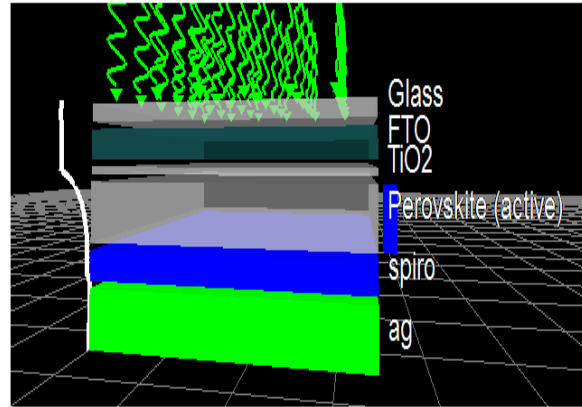


Figure 2. Planar heterojunction architecture of the studied solar cell

Table 1. Simulation parameters

Parameters	FTO	TiO_2	$\text{CH}_3\text{NH}_3\text{PbI}_3$	spiro-OMeTAD
Layer thickness (m)	$1e-7$ (variable)	$2.5e-8$ (variable)	$1e-7$ (variable)	$1e-7$ (variable)
Relative permittivity ϵ_r	3	9	3	3
Band gap energy (eV)	0	3.2	2.1	3.17
Electron affinity (eV)	4.7	4.26	3.7	2.05
Electron mobility ($\text{m}^2/\text{V.s}$)	$6.86e-07$	$20e-4$	$6.86e-07$	$2e-08$
Hole mobility ($\text{m}^2/\text{V.s}$)	$3.75e-02$	$10e-4$	$3.75e-02$	$2e-08$
Donor concentration (m^{-3})	$5e26$	$1e22$	$5e26$	0
Acceptor concentration (m^{-3})	$5e26$	0	$5e26$	$2e25$

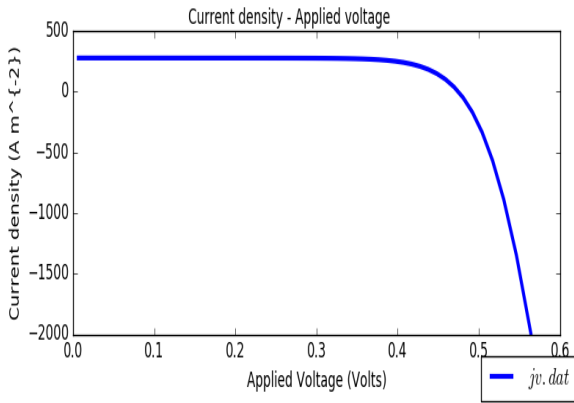


Figure 3. J-V characteristics for initial layer values

III. Results and discussion

Optimization method used in our simulation is to fix all parameters and modify one by one until we have the parameters that gives maximal PCE. In Figure 4 is presented the curve of effect of perovskite layer thickness on PCE.

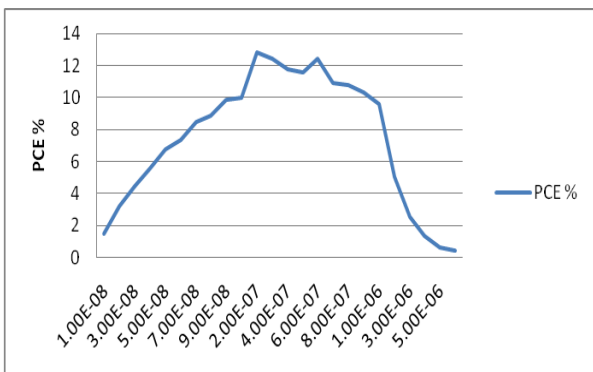


Figure 4. Effect of $\text{CH}_3\text{NH}_3\text{PbI}_3$ layer thickness on PCE

From Figure 4 we can note that a perovskite layer thickness of 2×10^{-7} m gives the maximal value of PCE which is 12.83 %, with a fill factor of 74.79 %, an open-circuit voltage of 0.47 V and a short-circuit density of current of -370 A/m^2 .

We fix the $\text{CH}_3\text{NH}_3\text{PbI}_3$ layer thickness on 2×10^{-7} m and we change the FTO layer thickness to obtain curve in Figure 5.

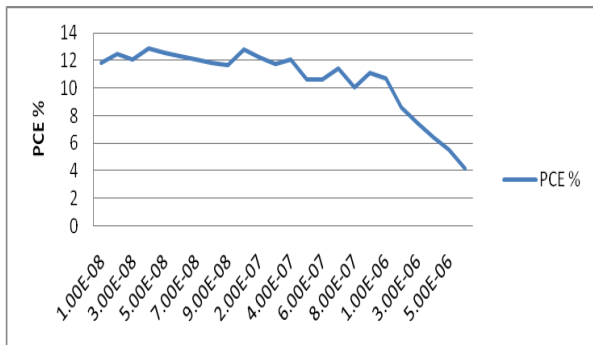


Figure 5. Effect of FTO layer thickness on PCE

From Figure 5 we obtained a maximal value of PCE which is 12.90 % corresponding on FTO layer thickness of 4×10^{-8} m, with a fill factor of 74.79 %, an open-circuit voltage of 0.47 V and a short-circuit density of current of -372 A/m^2 .

By setting FTO layer thickness to 4×10^{-8} m and changing the spiro-OMeTAD layer thickness we obtained curve in Figure 6.

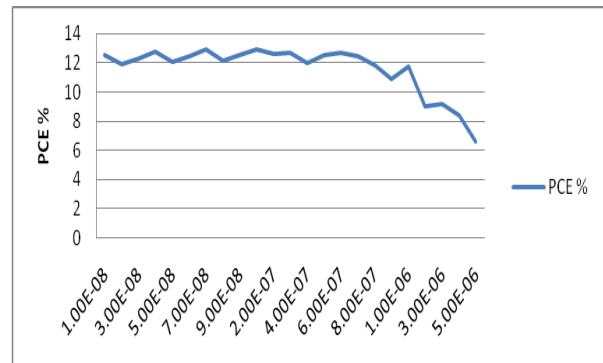


Figure 6. Effect of spiro-OMeTAD layer thickness on PCE

In Figure 6 we can note that the maximal PCE is 12.90 % in the spiro-OMeTAD layer thickness of 10^{-7} m with a fill factor of 74.79 %, an open-circuit voltage of 0.47 V and a short-circuit density of current of -372 A/m^2 .

When spiro-OMeTAD layer thickness is set to 10^{-7} m and changing of TiO_2 layer thickness we obtained curve in Figure 7.

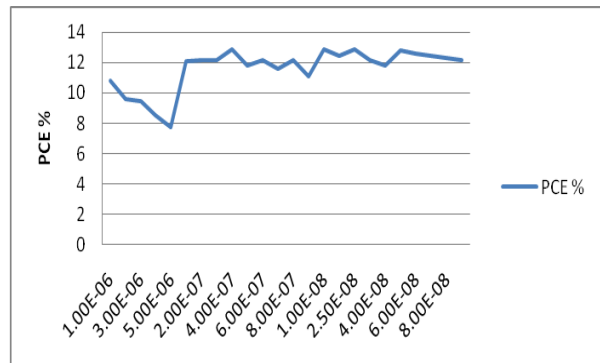


Figure 7. Effect of TiO_2 layer thickness on PCE

Curve of Figure 7 shows that Maximal PCE of 12.9 % is obtained in TiO_2 layer thickness of 2.5×10^{-8} m, where fill factor is 74.79 %, open-circuit voltage is 0.47 V and short-circuit density of current is -372 A/m^2 .

In Figure 4 to Figure 7 is presented different layer thickness effect on PCE for a $\text{CH}_3\text{NH}_3\text{PbI}_3$ based planar heterojunction solar cell where we saw that efficiency increased from 9.96 % in initial parameters to 12.9 % with optimized parameters.

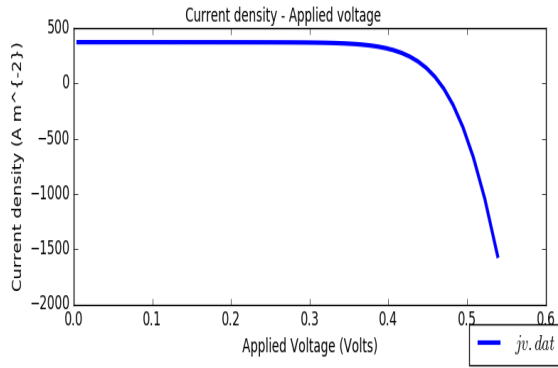


Figure 8. J-V characteristics for optimized layer values

In Figure 8 above we can see J-V characteristic of the studied solar cell with optimized parameters.

IV. Conclusion

Perovskite power conversion efficiency was analyzed using the GPVDM solar cell software simulation. Results indicate that a good choice of layer thickness of different materials used in the solar cell increases considerably the PCE ratio. From Simulation results is found that an improvement of 2.94 % is made by setting layer thickness of FTO to 4×10^{-8} m, of TiO₂ to 2.5×10^{-8} m, of Perovskite to 2×10^{-7} m and of spiro-OMeTAD to 10^{-7} m. Further PCE enhancements can be done by changing layer structure and materials.

V. Nomenclature

ϵ_0 is the permittivity of free space
 ϵ_r is the relative permittivity
 ϕ is the voltage profile
 q is the elementary charge on an electron
 n is the free electron concentration
 p is the free hole concentration
 J_n is the electron current flux density
 J_p is the hole flux density
 μ_c is the electron mobility
 μ_h is the hole mobility
 E_c is the free electron mobility edge
 E_v is the free hole mobility edge
 D_n is the electron diffusion coefficient
 D_p is the hole diffusion coefficient
 R_n is the net recombination rate for electrons
 R_p is the net recombination rate for holes
 G is the free carrier generation rate

References

- [1] Akihiro Kojima, Kenjiro Teshima, Yasuo Shirai and Tsutomu Miyasaka, Organometal halide perovskites as visible-light sensitizers for photovoltaic cells, *Journal of the American Chemical Society*, Vol. 131, no. 17, 2009, pp. 6050-6051.
- [2] J.-H. Im, C.-R. Lee, J.-W. Lee, S.-W. Park, and N.-G. Park, 6.5% efficient perovskite quantum-dot-sensitized solar cell, *Nanoscale*, vol. 3, no. 10, 2011; pp. 4088-4093.
- [3] M. A. Green, A. Ho-Baillie, and H. J. Snaith, The emergence of perovskite solar cells, *Nature Photonics*, vol. 8, no. 7, 2014, pp. 506-514.
- [4] B. Conings, L. Baeten, T. Jacobs, R. Dera, J. Dhaen, J. Manca, and H.G. Boyen, An easy-to-fabricate lowtemperature TiO₂ electron collection layer for high efficiency planar heterojunction perovskite solar cells, *APL Materials*, vol. 2, no. 8, 2014, pp. 081505.
- [5] R. Service, Perovskite solar cells keep on surging. *Science (New York, NY)*, vol. 344, no. 6183, 2014, pp 458.
- [6] M. Peplow, The perovskite revolution [news], *Spectrum, IEEE*, vol. 51, no. 7, 2014, pp. 16-17.
- [7] NREL chart 2018, 2018.
- [8] Roderick C. I. MacKenzie, Thomas Kirchartz, George F. A. Dibb, and Jenny Nelson, Modeling Nongeminate Recombination in P3HT:PCBM Solar Cells, *J. Phys. Chem. C*, Vol. 115, no. 19, 2011, pp 9806-9813.
- [9] R. Hanfland, M.A. Fischer, W. Brütting, U. Würfel, R.C.I. MacKenzie, The physical meaning of charge extraction by linearly increasing voltage transients from organic solar cells, *Appl. Phys. Lett.*, Vol. 103, no. 6, 2013, pp 063904.
- [10] F. Deschler, D. Riedel, B. Ecker, E. von Hauff, E. Da Como, R.C.I. MacKenzie, Increasing organic solar cell efficiency with polymer interlayers, *Phys. Chem. Chem. Phys.*, Vol. 15, no. 3, 2012, pp 764-769.
- [11] R.C.I. MacKenzie, C.G. Shuttle, M.L. Chabiny, J. Nelson, Extracting microscopic device parameters from transient photocurrent measurements of P3HT:PCBM solar cells, *Adv. Energy Mater.*, Vol. 2, no. 6, 2012, pp 662-669.
- [12] Umari, PP., E. Mosconi, and F. De Angelis, Relativistic GW calculations on CH₃NH₃PbI₃ and CH₃NH₃SnI₃ perovskites for solar cell applications, *Scientific reports*, Vol. 4, 2014, pp. 4467.
- [13] Qing-Yuan Chen, Y.H., Peng-Ru Huang, Tai Ma, Chao Cao, Yao He, Electronegativity explanation on the efficiency-enhancing mechanism of the hybrid inorganic-organic perovskite ABX₃ from first-principles study, *Chin. Phys. B*, Vol. 25, no. 2, 2015, pp. 27104-027104.
- [14] Noel, N.K., et al., Lead-free organic-inorganic tin halide perovskites for photovoltaic applications, *Energy & Environmental Science*, Vol. 7, no. 9, 2014, pp. 3061-3068.
- [15] Hao, F., et al., Lead-free solid-state organic-inorganic halide perovskite solar cells, *Nature Photonics*, Vol. 8, no. 6, 2014, pp. 489.
- [16] Minemoto, T. and M. Murata, Theoretical analysis on effect of band offsets in perovskite solar cells, *Solar Energy Materials and Solar Cells*, Vol. 133, 2015, pp. 8-14.
- [17] Kemp, K.W., et al., Interface recombination in depleted heterojunction photovoltaics based on colloidal quantum dots, *Advanced Energy Materials*, Vol. 3, no. 7, 2013, pp. 917-922.
- [18] Minemoto, T. and M. Murata, Device modeling of perovskite solar cells based on structural similarity with thin film inorganic semiconductor solar cells, *Journal of applied physics*, Vol. 116, no. 5, 2014, pp. 054505.

- [19] Minemoto, T. and M. Murata, Impact of work function of back contact of perovskite solar cells without hole transport material analyzed by device simulation, *Current Applied Physics*, Vol. 14, no. 11, 2014, pp. 1428-1433.
- [20] Liu, F., et al., Numerical simulation: toward the design of high-efficiency planar perovskite solar cells, *Applied Physics Letters*, Vol. 104, no. 25, 2014, pp. 253508.
- [21] Hui-Jing Du, W.-C.W., Jian-Zhuo Zhu, Device simulation of lead-free $\text{CH}_3\text{NH}_3\text{SnI}_3$ perovskite solar cells with high efficiency, *Chin. Phys. B*, Vol. 25, no. 10, 2016, pp. 108802-108802.
- [22] Ball, J.M., et al., Optical properties and limiting photocurrent of thin-film perovskite solar cells, *Energy & Environmental Science*, Vol. 8, no. 2, 2014, pp. 602-609.